



Unraveling the Role of Cytochrome P450 as a Key Regulator Lantipeptide Production in *Streptomyces globisporus*

Da-Ran Kim^{1†}, Su In Lee^{2†}, and Youn-Sig Kwak^{1,2*}

¹Research Institute of Life Science, Gyeongsang National University, Jinju 52828, Korea

²Division of Applied Life Science (BK21Plus), Gyeongsang National University, Jinju 52828, Korea

(Received on August 27, 2023; Revised on September 20, 2023; Accepted on September 20, 2023)

The aim of this study was to investigate the regulation of lantipeptide production in *Streptomyces globisporus* SP6C4, which produces the novel antifungal lantipeptides conprimycin and grisin, and to identify the role of cytochrome P450 (P450) in its regulation. To investigate the regulation of lantipeptide production, we created gene deletion mutants, including $\Delta P450$, $\Delta tsrD$, $\Delta lanM$, $\Delta P450\Delta tsrD$, and $\Delta P450\Delta lanM$. These mutants were characterized in terms of their morphology, sporulation, attachment, and antifungal activity against *Fusarium oxysporum*. The gene deletion mutants showed distinct characteristics compared to the wild-type strain. Among them, the $\Delta P450\Delta lanM$ double mutant exhibited a recovery of antifungal activity against *F. oxysporum*, indicating that P450 plays a significant role in regulating lantipeptide production in *S. globisporus* SP6C4. Our findings highlight the significant role of P450 in the regulation of lantipeptide production and morphological processes in *S. globisporus*. The results suggest a potential link between P450-mediated metabolic pathways and the regulation of growth and secondary metabolism in SP6C4, thereby highlighting

P450 as a putative target for the development of new antifungal agents.

Keywords : biological control, cytochrome P450, *Fusarium oxysporum*, *Streptomyces*

Actinomycetes, renowned for their ability to synthesize diverse bioactive compounds, have found applications in agriculture as microbial biocontrol agents (Chaiharin et al., 2020). Among the phylum Actinobacteria, *Streptomyces* is the largest genus, characterized by gram-positive bacteria with high G-C content. *Streptomyces* species are known for their extensive pharmacological activities and natural ability to produce industrially relevant natural products (Mahdi et al., 2022). Notably, they produce intriguing secondary metabolites such as alkaloids, flavones, macrolides, terpenoids, and polyketides, exhibiting antibacterial, antifungal, and anticancer properties (Genilloud, 2017). These secondary metabolites have previously been considered potential crop protection agents due to their antimicrobial, insecticidal, and herbicidal activities (Shi et al., 2019).

The antifungal activity of *Streptomyces* is multifaceted and can be attributed to a variety of mechanisms. *Streptomyces* is known to secrete biological antimicrobial substances, such as enzymes, polyketides, peptides, and other active substances, that interfere with the survival and growth of fungal cells. This secretion of antimicrobial substances allows *Streptomyces* to inhibit the growth of other microbes, which it perceives as competitors in its environment (Nguyen et al., 2021). In addition to the secretion of antimicrobial substances, *Streptomyces* can also exhibit antifungal activity by attacking the cell walls of fungi. Fungal cell walls play a critical role in their survival and growth, and when *Streptomyces* destroys these cell walls, it becomes difficult for the fungi to survive and grow (Jung

[†]These authors contributed equally to this work.

*Corresponding author.

Phone) +82-55-772-1922, FAX) +82-55-772-1929

E-mail) kwak@gnu.ac.kr

ORCID

Youn-Sig Kwak

https://orcid.org/0000-0003-2139-1808

Handling Editor : Hyong Woo Choi

© This is an Open Access article distributed under the terms of the Creative Commons Attribution Non-Commercial License (<http://creativecommons.org/licenses/by-nc/4.0>) which permits unrestricted noncommercial use, distribution, and reproduction in any medium, provided the original work is properly cited.

et al., 2018). Furthermore, *Streptomyces* can regulate its antifungal activity in response to specific environmental conditions. It can modulate or express its antifungal activity depending on factors such as nutrient conditions, temperature, pH, and other environmental cues (Romero-Rodriguez et al., 2015). Gene expression also plays a role in regulating the various antifungal mechanisms of *Streptomyces*, including antimicrobial substance secretion, cell wall attack, and physiological regulation. It is important to note that the antifungal activity of *Streptomyces* may not solely rely on a single mechanism, but rather multiple mechanisms that work together. For instance, *Streptomyces* can exhibit antifungal effects through a combination of secreting various active substances, attacking cell walls, and engaging in biological competition with competitors (Challis and Hopwood, 2003). This multifaceted approach suggests that *Streptomyces* utilizes a range of mechanisms to effectively exhibit antifungal activity. The antifungal activity of *Streptomyces* can be attributed to various mechanisms, including the secretion of antimicrobial substances, cell wall attack, physiological regulation, and gene expression control. These mechanisms work in concert to provide *Streptomyces* with its antifungal properties, allowing it to effectively inhibit the growth of other fungi in its environment.

A negative correlation was observed between the reduction in the population of core *Streptomyces*, particularly the key microbe *S. globisporus* SP6C4, and the loss of diversity. This correlation was observed in the context of a major anthosphere disease, specifically gray mold caused by *Botrytis cinerea* (Kim et al., 2019a). The analysis of the *S. globisporus* SP6C4 genome revealed the presence of several antifungal genes, including NRPS-PKS, PKS, ribosomal protein synthase-lantipeptide, and thiopeptide genes (Kim and Kwak, 2021). These functional metabolites are regulated by various transcription factors, such as the *whi* family, *TetR*, *sigH*, and *P450*. P450 (CYP or CYP-like) enzymes have diverse functions in *Streptomyces* growth, including the production of secondary metabolites, and exhibit a wide range of types within the bacterial system (Kaiser and Stoddard, 2011; Rebets et al., 2018). The P450 enzymes are also found in many types of organisms, including humans, insects, plants, fungi, bacteria, and archaea (Cho et al., 2019; Ngcobo et al., 2023). However, the structure and functions of P450 enzymes are still not fully understood, as they exhibit complex and diverse potentials (Guengerich, 2001; Han et al., 2015). Although genomic techniques have revealed the types of P450, their roles in *Streptomyces* metabolism remain unclear (Malinga et al., 2022). In this study, we investigated the P450-related re-

sponse in the metabolic pathway of *S. globisporus* P6C4. Our findings provide insights into the key regulators that can switch on the production of metabolites in the plant protection microbial strain.

Materials and Methods

The similarity of the P450 gene on *Streptomyces*. The chromosome of *S. globisporus* SP6C4 was accessed on the NCBI genome database BVBR (accession no. LWMQ00000000) and RAST server (version 2.0). Multiple sequence alignment at the gene level was performed using Clustal Omega (<https://www.ebi.ac.uk/Tools/msa/clustalo/>), and a phylogenetic tree was constructed using MEGA 11 with the maximum likelihood method. Domain and functional characterization at the protein level was carried out using the Conserved Domain Database (CDD) provided by NCBI. In secondary metabolite annotation at antiSMASH (version 6.0)

CRISPR/Cas9 mutagenesis. The *S. globisporus* SP6C4 genome was previously reported by Kim et al. (2019b), and a P450 gene was predicted using the RAST server (version 2.0) and antiSMASH (version 6.0). The gene was targeted for deletion using the CRISPR/Cas9 system with the pCRISPOmyces-2 plasmid. Gene-specific primers were designed for the left arm (LA) and right arm (RA) of the gene. Two fragments were amplified by polymerase chain reaction (PCR) in step I, using bacterial chromosome DNA at a concentration of 1 µg/µl, under the following conditions: initial denaturation at 98°C for 10 min, followed by 30 cycles of denaturation at 98°C for 1 min, annealing at 52-58°C for 30 s (depending on the respective primer melting temperature), elongation at 72°C for 30 s, and final extension at 72°C for 5 min. In step II, the LA and RA fragments (300 ng/µl each) were linked by PCR, with initial denaturation at 98°C for 30 s, followed by 5 cycles of denaturation at 98°C for 8 s, annealing at 50°C for 30 s, elongation at 72°C for 30 s, and extension at 72°C for 5 min. In step III, the homologous regions were amplified using the p450LA-F primer and p450RA-R primer (the PCR conditions were similar to step I, with the annealing temperature, changed to 60°C). PCR reactions were performed using an MJ Research PTC-200 thermal cycler (Bio-Rad, Hercules, CA, USA), and the PCR products were loaded on a 1% agarose gel. The amplicons were purified using the Expin GelSV kit (Gene All, Seoul, Korea) and eluted in 30 µl EB buffer. The T-vector ligation also requires A-tailing using 100 mM of dATP (NEB, Ipswich, MA, USA)

at 70°C for 30 min, followed by elution in 15 µl EB buffer. The purified solution was then ligated to a pGEM-T easy vector (Promega, Madison, WI, USA). After ligation, the pGEM-T easy vector was added to a homologous fragment selected by the blue/white colony method, and the mixture was transformed into *Escherichia coli* DH5α cells. The selective media used was LB (Luria broth; 30 g; agar, 20 g per liter) supplemented with ampicillin (100 µg/ml) and X-gal (40 µg/ml). A white colony was cultured in 5 ml of LB broth for 16 h at 37°C, and the plasmid was extracted using the Dokdo Mini-prep Kit (ELPIS-Biotech, Daejeon, Korea). Two different plasmids, the homologous ligated pGEM-T easy vector, and pCRISPomyces-gRNA were cut with *Xba*I (NEB) and ligated at a 1:3 backbone-to-insert ratio at 16°C overnight. The gRNA was cloned into pBHA (2,002 bp), and pCRISPomyces-2 was cut with *Bbs*I (NEB). The linear pCRISPomyces-2 and gRNA fragments were then ligated using T4 ligase (NEB). The final construction, pCRISPomyces-gRNA-homologous, was transformed into *E. coli* ET12567 containing pUZ8002 for conjugation with *Streptomyces*. In this step, the selection was performed on LB agar containing kanamycin (30 µg/ml), chloramphenicol (25 µg/ml), and apramycin (50 µg/ml). Prior to conjugation, the *E. coli* ET12567 cells containing pUZ8002 and the final construction were cultured in 10 ml of LB broth with the three antibiotics at 37°C for 9 h with shaking at 150 rpm. The cells were then gently washed with 10 ml of LB broth, followed by centrifugation (1,914 ×g for 15 min), and resuspended in 500 µl of LB broth. The bacterial spore stock (OD_{600nm}: 0.6, 10⁹ cfu/ml) was generated by mixing 500 µl of 2XYT medium with SP6C4 spore stock and *E. coli* cell and incubating at 50°C for 10 min, followed by cooling down and thorough mixing by pipetting. The mixture was then spread on MS agar (mannitol, 20 g; soya, 20 g; agar, 20 g per liter) and incubated for 16 h at 30°C. After 16 h, the plates were overlaid with antibiotics apramycin (50 µg/ml) and nalidixic acid (25 µg/ml) and air dried for 1 h. The conjugation colonies were transferred twice onto MS agar containing apramycin (50 µg/ml). All primers related to mutagenesis, gRNA sequences, and strain information are listed in Supplementary Tables 1 and 2.

Phenotypic analysis of mutants. All phenotypic assays were performed using the wild-type SP6C4 strain and its mutants. Spore stocks were cultured on MS agar plates for 10 days at 28°C, and sterilized cotton balls were added to 10-ml syringes to collect spores on media with 1 ml of ddH₂O. The filtered spore stock was detected at OD_{600nm}

as 0.6 (10⁶ cfu/ml) and stored at -20°C with 20% glycerol stock.

For the attachment assay, bacteria were cultured in 10 mL of PDK broth (containing 10 g peptone and 10 g potato dextrose per liter) for 7 days at 28°C without shaking. Then, 5 µl of SP6C4 strain or its mutants' spore stock was injected into a test tube ($n = 7$) containing the broth media. The tube was discarded from the broth media using a pipette, and 10 ml of 1% crystal violet was added to stain the tube for 15 min at room temperature. Subsequently, the tube was washed twice with 70% ethanol to remove the unstained dye.

The bacterial growth curve was determined by measuring the optical density at 600 nm over a 24-h period. For the sporulation assay, 10 µl of SP6C4 stain or its mutant spore stock was added to minimal media (L-asparagine 0.5 g, K₂HPO₄ 0.5 g, MgSO₄·7H₂O 0.2 g, FeSO₄·7H₂O 0.01 g, glucose 10 g, agar 15 g per liter, adjusted the pH 7.2) in a 96-well plate. The plate was then incubated at 28°C with shaking at 150 rpm for 5 days, with a sample size of $n = 7$.

The sporulation assay was performed using four different types of media: MS (mannitol 20 g, soya flour 20 g, agar 20 g per liter), PDK (peptone 10 g, potato dextrose broth 20 g, agar 20 g per liter), TSA (tryptic soya broth 25 g, agar 20 g per liter), and minimal media (L-asparagine 0.5 g, K₂HPO₄ 0.5 g, MgSO₄·7H₂O 0.2 g, FeSO₄·7H₂O 0.01 g, glucose 10 g, agar 15 g per liter, adjusted the pH 7.2). The media were dried at room temperature for 1 h, and then 2 µl of SP6C4 and mutant spore stock was spotted onto the media. The plates were incubated at 28°C for 10 days, with a sample size of $n = 5$. Sporulation was assessed at 24 h, 48 h, and 72 h.

Antifungal activity and plant assay. The antifungal activity was evaluated using PDK (peptone 10 g, potato dextrose broth 20 g, agar 20 g per liter) agar plates. Five microliters of spore stock were dotted at two sites and treated in a line 3 cm long from the center. After 3 days, *Fusarium oxysporum* f. sp. *lycopersici*, a cultured plant pathogen, was inoculated at the center of the plant using a 4-mm diameter cork bore and needle ($n = 7$). Seven days later, the antifungal activity was assessed based on the size of the inhibition zone, following the methods described by Cha et al. (2016) and Kim et al. (2019b).

Tomato seeds (cv. Heinz) were surface sterilized by washing with 1% NaOCl and 70% ethanol for 30 s each, followed by two washes with distilled water, and dried in a biosafety cabinet for 30 min. The surface-sterilized seeds were germinated on wetted cotton within a 9-cm diameter

petri dish for 3 days. The germinated seeds were then transferred to 9-cm plastic pots and cultured for up to 2 weeks under conditions of 60% relative humidity, 16-h light, and 8-h dark, with a temperature maintained at 28–32°C. Two weeks later, SP6C4 bacterial cultured cells (10^6 cfu/ml) and their mutants were drenched on each plant, with the culture containing a final concentration of 0.1% v/v of CMC (carboxyl-methylcellulose). Starting from 7 days after the addition of bacterial suspension, *F. oxysporum* f. sp. *lycospersici* was inoculated on the tomato plants, and the pathogen was cultured as chlamydospores in 1% oatmeal and soil inoculum. The chlamydospore density of the pathogen was calculated using a hemocytometer, and it was found to be 10^5 spores/g. The disease index was recorded during the growth stage, and each treatment had 15 plant replications.

Total RNA extraction and quantitative real time polymerase chain reaction. The quantitative real time polymerase chain reaction (qRT-PCR) primers used in this study were obtained from Kim and Kwak (2021). Total RNA was extracted twice: first at the stage of aerial hyphal formation for the expression of *tsrD* gene (48 h), and second after aerial hyphae formation for the expression of *lanM* gene (72 h). Bacterial cells were ground with liquid nitrogen, and the resulting pellet was stored at -80°C . RNA extraction was carried out using the TRIzol method and RNeasy Mini kit (Qiagen, Hilden, Germany) for column purification. The extracted RNA was then synthesized into cDNA using the ReverTraAce- α - R cDNA Synthesis Kit (TOYOBO, Osaka, Japan), and qRT-PCR was performed using the CFX96 Touch Real-Time PCR Detection System (Bio-Rad). Five replicates were performed for each mutant cDNA library in the qRT-PCR analysis.

Statistical analyses. The statistical analyses of all graphs were conducted using ANOVA, *t*-test. If the data did not meet the assumptions of normality and equal variance, they were analyzed using ANOVA *post-hoc* tests were performed using Tukey's honestly significant difference (Konietzke et al., 2008; Munzel and Hothorn, 2001). The graphs were visualized using ggplot2 from the R software package.

Results and Discussion

S. globisporus SP6C4 has been reported to produce two different antifungal compounds against the pathogen *Fusarium oxysporum* (Kim et al., 2019b). The biosynthesis genes for these compounds have been identified as *tsrD*,

which produces conprimycin (Cha et al., 2016), and *lanM*, which produces gisin (Kim et al., 2019b). These antifungal compounds belong to the lantipeptide group, which is macrocyclic in structure and heat-stable molecule. Lantipeptides are commonly found in gram-positive bacteria such as *Bacillus* and *Streptomyces* (Mnguni et al., 2020; Repka et al., 2017; Zhang et al., 2015). The biosynthetic enzymes for lantipeptides are encoded in gene clusters, including lantipeptide-CYP152A1 and thiopeptide-CYP119, which are part of specific lantipeptide biosynthesis pathways (Gober et al., 2017).

P450 clusters in SP6C4 strain. The functions and structures of *Streptomyces* species cytochrome P450 enzymes have been reported (Cho et al., 2019). These enzymes, also known as P450d CYP, are involved in various catalytic, metabolic, and biosynthetic activities, as well as in toxicity and drug metabolism (Guengerich, 2001). The compared region for the P450 cluster in *S. globisporus* SP6C4 was analyzed using Seed Viewer version 2.0. The cutoff for similarity in this cluster was set at more than 40% identity. Multiple P450 biosynthesis genes of *Streptomyces* spp. were aligned using MEGA11 and a phylogenetic tree was generated using maximum likelihood (Supplementary Fig. 1). The results revealed that the P450 gene of SP6C4 belonged to a distinct group compared to other species, such as *S. albus*, *S. baarnensis*, and *S. anulatus*, and showed similarity only to *S. griseus*. The strain SP6C4 showed similarity to *Streptomyces* groups, specifically *S. griseus* NBRC13350 (E-value: 0). Additionally, it showed similarity to the class of Actinomycetia, including Streptosporangium (E-value: 3.00E^{-124}), Thermomonospora (E-value: 8.00E^{-92}), and Mycobacterium (E-value: 1.00E^{-73}), as determined by PSI-BLAST (Supplementary Table 3).

The SP6C4 stain was found to have *melC1* and *melC2*

Table 1. P450 biosynthesis gene cluster in *Streptomyces globisporus* SP6C4

Rast annotation	BVBRC ^a	Omega gene similarity (%)	Omega protein similarity (%)
Putative tyrosinase	Tyrosinase (<i>melC1</i>)	99	100
Putative tyrosinase co-factor protein	<i>melC2</i>	99	99
Cytochrome P450 hydroxylase	P450	99	98

^aBacterial and Viral Bioinformatics Resource Center (<https://www.bv-brc.org/>).

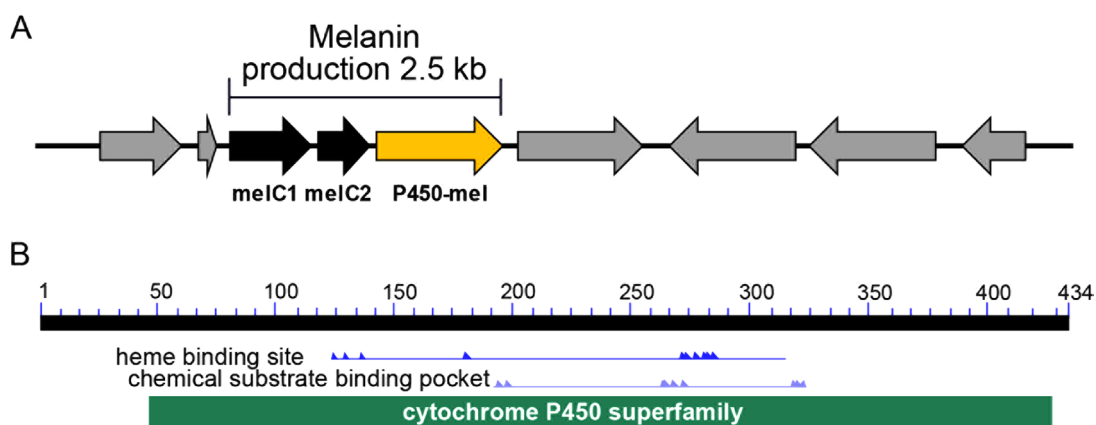


Fig. 1. Gene organization and function of the P450 clusters in *Streptomyces globisporus* SP6C4. (A) Gene arrangement of the melanin biosynthesis cluster, which includes the P450 enzyme, on the *S. globisporus* SP6C4 chromosome. (B) Domain search results from NCBI's Conserved Domain Database (CDD) showing the P450 enzyme domain region.

genes upstream of the P450 biosynthesis gene, and three different genes were aligned with DNA and protein levels using the NCBI database, showing more than 99% similarity (Table 1, Fig. 1A). Domain search revealed that SP6C4-P450 belonged to the cytochrome P450 (CYP) superfamily (cd00302) and CYP142-like (cd11033) (Fig 1B). These CYPs were found to have heme-binding sites associated with various oxidation reactions and exhibited diverse structural characteristics. Among the *Streptomyces* species, *S. coelicolor*, *S. avermitalis*, *S. velenzuelae*, *S. rapamycinicus*, *S. hygroscopicus*, and *S. peucetius* have the highest number of groups, including CYP105N1, CYP171A1, CYP107L1, CYP112A2, and CYP129A2, respectively (Cho et al., 2019; Lim et al., 2012). These groups belong to 144 P450 families and 377 P450 subfamilies (Moshoeshoe, 2019). Although the reactions catalyzed by these CYP enzymes have been reported, their participation in biological processes such as electron transfer, anti-functional compound synthesis, and oxidation, which may uncover additional functions, is still not fully understood (Han et al., 2015; Lee et al., 2016).

Disruption of P450 gene cluster and effects on attachment, bacterial growth, and sporulation. We annotated a number of P450 genes and conducted a comparative analysis of P450s at the SP6C4 genome level to validate their key role as secondary metabolite regulators. Twenty-three cytochrome genes were detected in the SP6C4 genome, including a putative melanin-related P450 gene, which showed low similarity to *Streptomyces* species at the protein level but high alignment with other Actinomycete classes at the gene level, with unassigned functions.

The gene cluster of *P450* was disrupted by a double homologous recombination process resulting in two mutants, $\Delta P450\Delta tsrD$ and $\Delta P450\Delta lanM$, where an antifungal biosynthesis gene (*tsrD* and *lanM*) was deleted in a two-step process, followed by the loss of the P450 enzyme. Phenotypic assays were performed for attachment, bacterial growth, and sporulation. In the attachment assay, crystal violet staining revealed that the wild type (WT) and $\Delta P450$ mutants showed a colored line in the glass tube, while the $\Delta P450\Delta tsrD$ mutant exhibited a darker line (Fig. 2A). Other mutant lines $\Delta tsrD$, $\Delta lanM$, $\Delta P450$, and $\Delta P450\Delta lanM$ showed no attachment ability in glass tubes (Fig. 2A). Assays were conducted in 96-well plates for bacterial growth, and OD values were analyzed using the Gompertz model and rolling regression analysis. The mutant $\Delta P450\Delta tsrD$ exhibited an exponential growth rate with a maximum slope ($\mu = 0.4/1$ h) and 95% confidence intervals predicted (Fig. 2B). The growth rates of the WT and other mutant lines $\Delta tsrD$, $\Delta lanM$, $\Delta P450$, and $\Delta P450\Delta lanM$ were within the 95% confidence intervals, and the growth rate of $\Delta P450\Delta tsrD$ was higher (0.49-0.57/1 h) than that of $\Delta P450\Delta tsrD$ (Supplementary Fig. 2). Consequently, the exponential growth rate was determined by employing a rolling regression approach, and the slope of the linear regression between the optical density (OD_{600nm}) and time was utilized as the estimate for exponential growth. The sporulation test was performed using various media, ranging from high nutrient richness (MS, PDK, TSA) to low (minimal media) to mimic different *Streptomyces* growth conditions. The wild-type strain exhibited high sporulation across all media at 24 to 72 h (Fig. 2C). Among the mutant lines, $\Delta P450$, $\Delta lanM$, and $\Delta P450\Delta lanM$ showed good

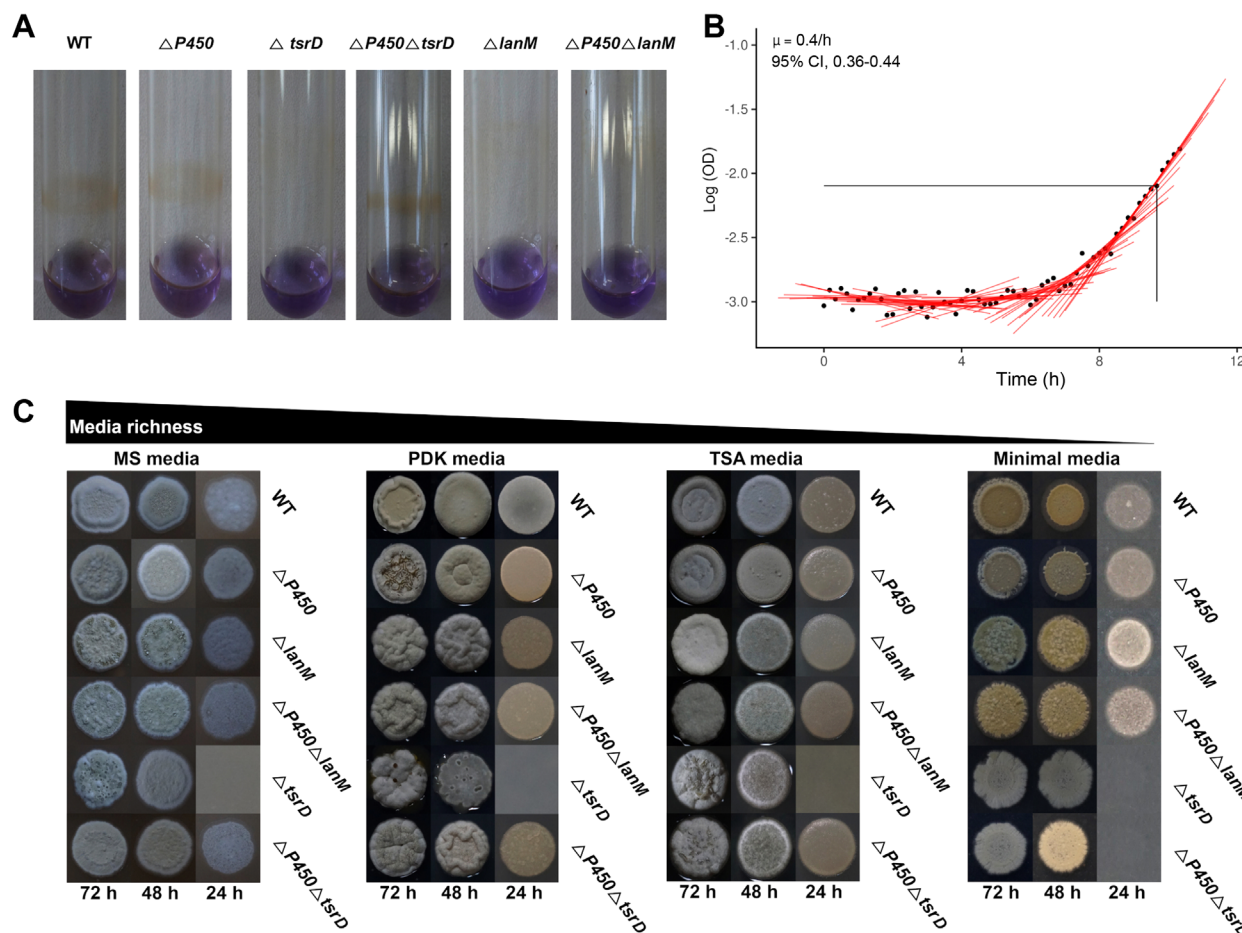


Fig. 2. Phenotypic characterization of strain SP6C4 on deleted mutant lines. (A) Ten microliters of bacteria were inoculated on PDK broth and incubated at 28°C for 7 days ($n = 5$). After 7 days, the medium was discarded, and the tube was washed twice with 70% ethanol. The tube was then cleaned and allowed to dry in a hood for 1 h. (B) Bacterial growth was assessed by adding cells to a 96-well plate containing minimal media broth and incubating at 28°C for 5 days with 150 rpm ($n = 7$). The OD value was calculated with the Gompertz linear regression model. CI, confidence interval. (C) Sporulation ability was monitored at 24 h to 72 h time points, with 10 μ l of spore stock inoculated at a concentration of 10^6 cfu/ml. The plate was incubated at 28°C for 10 days ($n = 5$).

sporulation in multiple types of media at different time points, while $\Delta tsrD$ did not show any sporulation at 24 h in any medium (Fig. 2C). However, the double knockout mutant $\Delta P450\Delta tsrD$ showed sporulation even at 24 h in rich media such as MS, PDK, and TSA (Fig. 2C). Therefore, the sporulation ability of $\Delta P450\Delta tsrD$ was found to be higher than that of $\Delta tsrD$. These changes in phenotypic characters are likely to affect secondary metabolite production, as *Streptomyces* undergoes a complex developmental life cycle involving mycelial growth and sporulation, and morphological differentiation is required for new activities (Bobek et al., 2014; McCormick and Flärth, 2012).

Recovery of antifungal activity in double deletion mutant against fungal pathogen. The strain SP6C4 exhibits

antifungal activity against the pathogen *Fusarium oxysporum* in strawberries (Kim et al., 2019b, 2021). This finding is consistent with the antifungal activity observed in the tomato pathogen *Fusarium oxysporum* f. sp. *lycopersici* (Kim et al., 2021). Mutagenesis lines showed differential activity against the pathogen, with $\Delta P450$ showing no significant difference compared to the WT, while signal mutants $\Delta tsrD$ and $\Delta lanM$ lost their antifungal ability (Fig. 3). Interestingly, one of the double deletion mutants, $\Delta P450\Delta tsrD$, showed regained inhibition of fungal growth against *F. oxysporum* f. sp. *lycopersici* (Fig. 3). Volatile tests using four fungal pathogens, including *Botrytis cinerea*, *F. oxysporum* f. sp. *fragariae*, *F. oxysporum* f. sp. *lycopersici*, and *Phytophthora fragariae*, showed no difference between WT and mutant lines (Supplementary Fig. 3).

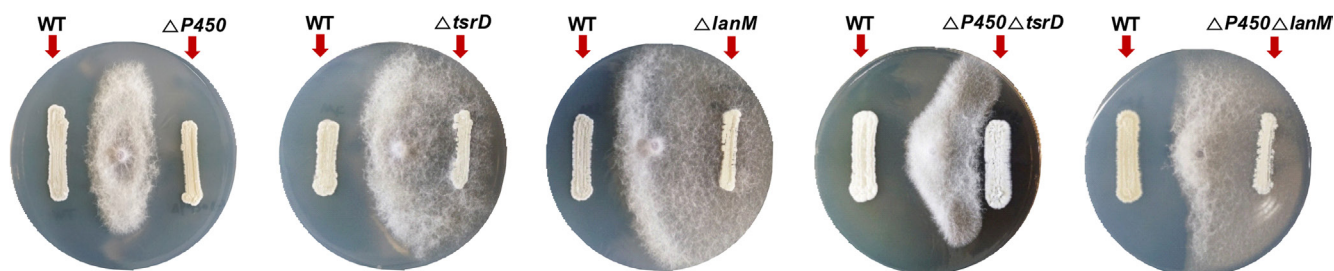


Fig. 3. Antifungal activity of SP6C4 and mutant lines against *Fusarium oxysporum* f. sp. *lycopersici*. Wild-type *Streptomyces globisporus* SP6C4, P450 deletion mutant, and double deleted mutants were tested for their antagonistic activity against the fungal pathogen. The bacterial stock was collected from MS media (mannitol 20 g; soya flour 20 g; agar 20 g per liter) using a 10-ml syringe and a sterilized cotton ball and inoculated onto PDK agar with 10 μ l of stock at OD600 0.6. After 3 days, an agar block (0.4 cm diam.) of the fungal pathogen was added to the center of the plate and incubated for 7 days at 28°C ($n = 7$).

In biocontrol assays using wild-type and mutant lines, a similar pattern was observed in the *in vitro* test results on agar plates. The disease index values ranged from 0 to 5, with WT and untreated showing a value of 0, $\Delta P450$ and

$\Delta P450\Delta tsrD$ showing a value of 1.2, which was not significantly different in Tukey's test (Fig. 4A, Supplementary Table 4). However, values higher than 3 were observed in $\Delta lanM$, $\Delta tsrD$, $\Delta P450\Delta lanM$, and all values were counted

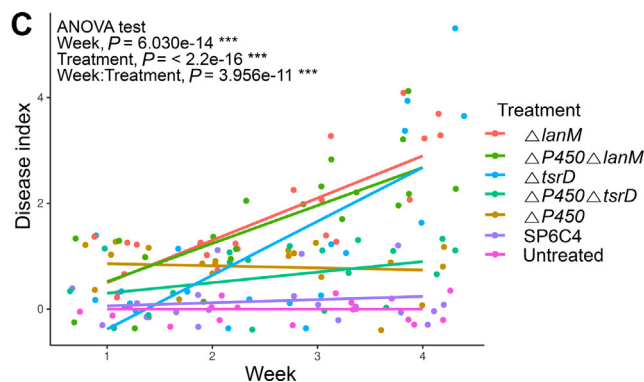
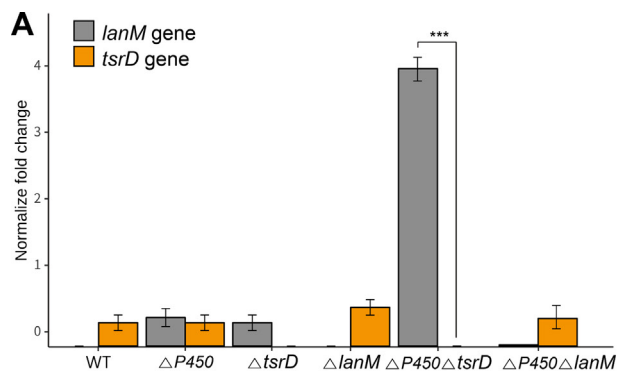


Fig. 4. Antifungal specific genes qRT-PCR and biocontrol assay in tomato. (A) Total RNA ($\leq 1 \mu$ g) was extracted from bacteria, and cDNA library was synthesized using the ReverTraAce- α - ® cDNA Synthesis Kit. The cDNA was then used as the template for the amplification of target genes *tsrD* and *lanM*, with normalization to a housekeeping gene and calculation of fold change ($n = 5$). Statistical significance was determined using the student's *t*-test. (B, C) Tomato plants were grown at the vegetative stage and drenched with 10 ml of bacterial stock with 0.1% CMC (v/v) and inoculated with chlamydospore stock (10^5 spores/g) on each plant with 10 ml. After 4 weeks, the disease index was calculated on a scale of 0 to 5 ($n = 15$), and linear regression ANOVA was performed.

after 4 weeks (Fig. 4A and B). The data was generated using a time serial model, which revealed significant differences in week intervals ($P = 6.030E^{-14}$) among the treatments ($P < 2.2E^{-16}$), and interactions between the two factors with a P -value of $3.956E^{-11}$ (Fig. 4A, Supplementary Fig. 4). This result indicates that the recovered antifungal activity in $\Delta P450\Delta tsrD$ can also be demonstrated in plants.

We elucidated the expression patterns of eight regions of biosynthetic genes, including *lanM* (grisin biosynthesis) and *tsrD* (conprimycin biosynthesis), as well as three types of *NRPS* and *PKS* genes, which were previously reported by Kim and Kwak (2021) as secondary metabolite-related genes in *S. globisporus* SP6C4. Among these genes, *lanM* showed a significant increase in expression with a fold change greater than 3 Log2 fold in the $\Delta P450\Delta tsrD$ mutant, indicating its key role in antifungal effects. In contrast, *tsrD* was not expressed in mutant lines, including $\Delta P450$, $\Delta P450\Delta lanM$, and $\Delta P450\Delta tsrD$ (Fig. 5C). When examining other secondary metabolite-related genes using Log2 fold change as a metric, the *NRPS* and *PKS* genes showed expression levels lower than 0 at 48 h in $\Delta P450$ and $\Delta P450\Delta lanM$ mutants (Supplementary Fig. 5A and B). The $\Delta P450\Delta tsrD$ mutant exhibited slightly increased expression at 48 h, but no significant upregulation, whereas at 72 h, *NRPS* and *PKS* genes showed 3-5 Log2 fold change in each mutant (Supplementary Fig. 5C). The key finding of this study was the antagonism assay, which unexpectedly showed that the $\Delta P450\Delta tsrD$ mutant regained antifungal activity against the pathogen. Furthermore, although the mechanism is unclear, the expression of *lanM* antifungal-related genes was upregulated in the $\Delta P450\Delta tsrD$ mutant.

Our results suggest that the enzyme P450-CYP142 is involved in the morphological processes of *S. globisporus* SP6C4, including antifungal activity. Specifically, we propose that P450-CYP142 acts as a repressor at the *lanM* gene under normal conditions, without specific signaling to favor. These findings highlight the significant role of the P450-CYP142 enzyme in modulating the morphological response of *S. globisporus* SP6C4, as well as its contribution to the strain's antifungal ability. These results imply the potential involvement of P450-CYP142-mediated metabolic pathways in shaping the growth and secondary metabolism of *S. globisporus* SP6C4, thus underscoring its relevance as a putative target for the development of novel antifungal agents.

Conflicts of Interest

No potential conflict of interest relevant to this article was

reported.

Acknowledgments

This work was supported by the National Research Foundation of Korea (NRF) grant funded by the Korea government (MIST) [2020R1A2C2004177].

Electronic Supplementary Material

Supplementary materials are available at The Plant Pathology Journal website (<http://www.ppjonline.org/>).

References

- Bobek, J., Strakova, E., Zikova, A. and Vohradsky, J. 2014. Changes in activity of metabolic and regulatory pathways during germination of *S. coelicolor*. *BMC Genomics* 15:1173.
- Cha, J.-Y., Han, S., Hong, H.-J., Cho, H., Kim, D., Kwon, Y., Kwon, S.-K., Crüsemann, M., Lee, Y. B., Kim, J. F., Giaever, G., Nislow, C., Moore, B. S., Thomashow, L. S., Weller, D. M. and Kwak, Y.-S. 2016. Microbial and biochemical basis of a fusarium wilt-suppressive soil. *ISME J.* 10:119-129.
- Chaihan, M., Theantana, T. and Pathom-Aree, W. 2020. Evaluation of biocontrol activities of *Streptomyces* spp. against rice blast disease fungi. *Pathogens* 9:126.
- Challis, G. L. and Hopwood, D. A. 2003. Synergy and contingency as driving forces for the evolution of multiple secondary metabolite production by *Streptomyces* species. *Proc. Natl. Acad. Sci. U. S. A.* 100:14555-14561.
- Cho, M.-A., Han, S., Lim, Y.-R., Kim, V., Kim, H. and Kim, D. 2019. *Streptomyces* cytochrome P450 enzymes and their roles in the biosynthesis of macrolide therapeutic agents. *Biomol. Ther.* 27:127-133.
- Genilloud, O. 2017. Actinomycetes: still a source of novel antibiotics. *Nat. Prod. Rep.* 34:1203-1232.
- Gober, J. G., Ghodge, S. V., Bogart, J. W., Wever, W. J., Watkins, R. R., Brustad, E. M. and Bowers, A. A. 2017. 450-mediated non-natural cyclopropanation of dehydroalanine-containing thiopeptides. *ACS Chem. Biol.* 12:1726-1731.
- Guengerich, F. P. 2001. Analysis and characterization of enzymes and nucleic acids. In: *Principles and methods of toxicology*, ed. by A. W. Hayes, pp. 1625-1687. Taylor & Francis, Philadelphia, PA, USA.
- Han, S., Pham, T.-V., Kim, J.-H., Lim, Y.-R., Park, H.-G., Cha, G.-S., Yun, C.-H., Chun, Y.-J., Kang, L.-W. and Kim, D. 2015. Functional characterization of CYP107W1 from *Streptomyces avermitilis* and biosynthesis of macrolide oligomycin A. *Arch. Biochem. Biophys.* 575:1-7.
- Jung, S. J., Kim, N. K., Lee, D.-H., Hong, S. I. and Lee, J. K. 2018. Screening and evaluation of *Streptomyces* species as a potential biocontrol agent against a wood decay fungus,

- Gloeophyllum trabeum*. *Mycobiology* 46:138-146.
- Kaiser, B. K. and Stoddard, B. L. 2011. DNA recognition and transcriptional regulation by the *whiA* sporulation factor. *Sci. Rep.* 1:156.
- Kim, D.-R., Cho, G., Jeon, C.-W., Weller, D. M., Thomashow, L. S., Paulitz, T. C. and Kwak, Y.-S. 2019a. A mutualistic interaction between *Streptomyces* bacteria, strawberry plants and pollinating bees. *Nat. Commun.* 10:4802.
- Kim, D.-R., Jeon, C.-W., Cho, G., Thomashow, L. S., Weller, D. M., Paik, M.-J., Lee, Y.-B. and Kwak, Y.-S. 2021. Glutamic acid reshapes the plant microbiota to protect plants against pathogens. *Microbiome* 9:244.
- Kim, D.-R., Jeon, C.-W., Shin, J.-H., Weller, D. M., Thomashow, L. and Kwak, Y.-S. 2019b. Function and distribution of a lantipeptide in strawberry fusarium wilt disease-suppressive soils. *Mol. Plant-Microbe Interact.* 32:306-312.
- Kim, D.-R. and Kwak, Y.-S. 2021. A genome-wide analysis of antibiotic producing genes in *Streptomyces globisporus* SP6C4. *Plant Pathol. J.* 37:389-395.
- Konietschke, F., Brunner, E. and Hothorn, L. A. 2008. Nonparametric relative contrast effects: asymptotic theory and small sample approximations. URL <https://rdrr.io/cran/nparcomp/man/nparcomp.html> [27 August 2023].
- Lee, C. W., Lee, J.-H., Rimal, H., Park, H., Lee, J. H. and Oh, T.-J. 2016. Crystal structure of cytochrome P450 (CYP105P2) from *Streptomyces peucetius* and its conformational changes in response to substrate binding. *Int. J. Mol. Sci.* 17:813.
- Lim, Y.-R., Hong, M.-K., Kim, J.-K., Doan, T. T. N., Kim, D.-H. Yun, C.-H., Chun, Y.-J., Kang, L.-W. and Kim, D. 2012. Crystal structure of cytochrome P450 CYP105N1 from *Streptomyces coelicolor*, an oxidase in the coelibactin siderophore biosynthetic pathway. *Arch. Biochem. Biophys.* 528:111-117.
- Mahdi, R. A., Bahrami, Y. and Kakaei, E. 2022. Identification and antibacterial evaluation of endophytic actinobacteria from *Luffa cylindrica*. *Sci. Rep.* 12:18236.
- Malinga, N. A., Nzuza, N., Padayachee, T., Syed, P. R., Karpoor-math, R., Gront, D., Nelson, D. R. and Syed, K. 2022. An unprecedented number of cytochrome P450s are involved in secondary metabolism in *Salinispora* species. *Microorganisms* 10:871.
- McCormick, J. R. and Flärdh, K. 2012. Signals and regulators that govern *Streptomyces* development. *FEMS Microbiol. Rev.* 36:206-231.
- Mnguni, F. C., Padayachee, T., Chen, W., Gront, D., Yu, J.-H., Nelson, D. R. and Syed, K. 2020. More P450s are involved in secondary metabolite biosynthesis in *Streptomyces* compared to *Bacillus*, *Cyanobacteria*, and *Mycobacterium*. *Int. J. Mol. Sci.* 21:4814.
- Moshoeshe, S. 2019. Comparative analysis of cytochrome P450 monooxygenases between the genera *Streptomyces* and *Mycobacterium*. Ph.D. thesis. Central University of Technology, Bloemfontein, South Africa.
- Munzel, U. and Hothorn, L. A. 2001. A unified approach to simultaneous rank tests procedures in the unbalanced one-way layout. *Biom. J.* 43:553-569.
- Ngcobo, P. E., Nkosi, B. V. Z., Chen, W., Nelson, D. R. and Syed, K. 2023. Evolution of cytochrome P450 enzymes and their redox partners in Archaea. *Int. J. Mol. Sci.* 24:4161.
- Nguyen, H. T. T., Park, A. R., Hwang, I. M. and Kim, J.-C. 2021. Identification and delineation of action mechanism of anti-fungal agents: reveromycin E and its new derivative isolated from *Streptomyces* sp. JCK-6141. *Postharvest Biol. Technol.* 182:111700.
- Rebets, Y., Tsohis, K. C., Guðmundsdóttir, E. E., Koepff, J., Wawiernia, B., Busche, T., Bleidt, A., Horbal, L., Myronovskiy, M., Ahmed, Y., Wiechert, W., Rückert, C., Hamed, M. B., Bilyk, B., Anné, J., Friðjónsson, Ó., Kalinowski, J., Oldiges, M., Economou, A. and Luzhetskyy, A. 2018. Characterization of sigma factor genes in *Streptomyces lividans* TK24 using a genomic library-based approach for multiple gene deletions. *Front. Microbiol.* 9:3033.
- Repka, L. M., Chekan, J. R., Nair, S. K. and van der Donk, W. A. 2017. Mechanistic understanding of lanthipeptide biosynthetic enzymes. *Chem. Rev.* 117:5457-5520.
- Romero-Rodriguez, A., Robledo-Casados, I. and Sánchez, S. 2015. An overview on transcriptional regulators in *Streptomyces*. *Biochim. Biophys. Acta* 1849:1017-1039.
- Shi, L., Wu, Z., Zhang, Y., Zhang, Z., Fang, W., Wang, Y., Wan, Z., Wang, K. and Ke, S. 2019. Herbicidal secondary metabolites from Actinomycetes: structure diversity, modes of action, and their roles in the development of herbicides. *J. Agric. Food Chem.* 68:17-32.
- Zhang, Q., Doroghazi, J. R., Zhao, X., Walker, M. C. and van der Donk, W. A. 2015. Expanded natural product diversity revealed by analysis of lanthipeptide-like gene clusters in Actinobacteria. *Appl. Environ. Microbiol.* 81:4339-4350.